

Search for the decay $D^0 \rightarrow \gamma\gamma$ and measurement of the branching fraction for $D^0 \rightarrow \pi^0\pi^0$

J. P. Lees,¹ V. Poireau,¹ E. Prencipe,¹ V. Tisserand,¹ J. Garra Tico,² E. Grauges,² M. Martinelli,^{3a,3b} D. A. Milanese,^{3a,3b} A. Palano,^{3a,3b} M. Pappagallo,^{3a,3b} G. Eigen,⁴ B. Stugu,⁴ L. Sun,⁴ D. N. Brown,⁵ L. T. Kerth,⁵ Yu. G. Kolomensky,⁵ G. Lynch,⁵ H. Koch,⁶ T. Schroeder,⁶ D. J. Asgeirsson,⁷ C. Hearty,⁷ T. S. Mattison,⁷ J. A. McKenna,⁷ A. Khan,⁸ V. E. Blinov,⁹ A. R. Buzykaev,⁹ V. P. Druzhinin,⁹ V. B. Golubev,⁹ E. A. Kravchenko,⁹ A. P. Onuchin,⁹ S. I. Serednyakov,⁹ Yu. I. Skovpen,⁹ E. P. Solodov,⁹ K. Yu. Todyshev,⁹ A. N. Yushkov,⁹ M. Bondioli,¹⁰ S. Curry,¹⁰ D. Kirkby,¹⁰ A. J. Lankford,¹⁰ M. Mandelkern,¹⁰ D. P. Stoker,¹⁰ H. Atmacan,¹¹ J. W. Gary,¹¹ F. Liu,¹¹ O. Long,¹¹ G. M. Vitug,¹¹ C. Campagnari,¹² T. M. Hong,¹² D. Kovalskyi,¹² J. D. Richman,¹² C. A. West,¹² A. M. Eisner,¹³ J. Kroseberg,¹³ W. S. Lockman,¹³ A. J. Martinez,¹³ T. Schalk,¹³ B. A. Schumm,¹³ A. Seiden,¹³ C. H. Cheng,¹⁴ D. A. Doll,¹⁴ B. Echenard,¹⁴ K. T. Flood,¹⁴ D. G. Hitlin,¹⁴ P. Ongmongkolkul,¹⁴ F. C. Porter,¹⁴ A. Y. Rakitin,¹⁴ R. Andreassen,¹⁵ M. S. Dubrovin,¹⁵ B. T. Meadows,¹⁵ M. D. Sokoloff,¹⁵ P. C. Bloom,¹⁶ W. T. Ford,¹⁶ A. Gaz,¹⁶ M. Nagel,¹⁶ U. Nauenberg,¹⁶ J. G. Smith,¹⁶ S. R. Wagner,¹⁶ R. Ayad,^{17,*} W. H. Toki,¹⁷ B. Spaan,¹⁸ M. J. Kobel,¹⁹ K. R. Schubert,¹⁹ R. Schwierz,¹⁹ D. Bernard,²⁰ M. Verderi,²⁰ P. J. Clark,²¹ S. Playfer,²¹ J. E. Watson,²¹ D. Bettoni,^{22a} C. Bozzi,^{22a} R. Calabrese,^{22a,22b} G. Cibinetto,^{22a,22b} E. Fioravanti,^{22a,22b} I. Garzia,^{22a,22b} E. Luppi,^{22a,22b} M. Menerato,^{22a,22b} M. Negrini,^{22a,22b} L. Piemontese,^{22a} R. Baldini-Ferroli,²³ A. Calcaterra,²³ R. de Sangro,²³ G. Finocchiaro,²³ M. Nicolaci,²³ S. Pacetti,²³ P. Patteri,²³ I. M. Peruzzi,^{23,†} M. Piccolo,²³ M. Rama,²³ A. Zallo,²³ R. Contri,^{24a,24b} E. Guido,^{24a,24b} M. Lo Vetere,^{24a,24b} M. R. Monge,^{24a,24b} S. Passaggio,^{24a} C. Patrignani,^{24a,24b} E. Robutti,^{24a} B. Bhuyan,²⁵ V. Prasad,²⁵ C. L. Lee,²⁶ M. Morii,²⁶ A. J. Edwards,²⁷ A. Adametz,²⁸ J. Marks,²⁸ U. Uwer,²⁸ F. U. Bernlochner,²⁹ M. Ebert,²⁹ H. M. Lacker,²⁹ T. Lueck,²⁹ P. D. Dauncey,³⁰ M. Tibbetts,³⁰ P. K. Behera,³¹ U. Mallik,³¹ C. Chen,³² J. Cochran,³² H. B. Crawley,³² W. T. Meyer,³² S. Prell,³² E. I. Rosenberg,³² A. E. Rubin,³² A. V. Gritsan,³³ Z. J. Guo,³³ N. Arnaud,³⁴ M. Davier,³⁴ D. Derkach,³⁴ G. Grosdidier,³⁴ F. Le Diberder,³⁴ A. M. Lutz,³⁴ B. Malaescu,³⁴ P. Roudeau,³⁴ M. H. Schune,³⁴ A. Stocchi,³⁴ G. Wormser,³⁴ D. J. Lange,³⁵ D. M. Wright,³⁵ I. Bingham,³⁶ C. A. Chavez,³⁶ J. P. Coleman,³⁶ J. R. Fry,³⁶ E. Gabathuler,³⁶ D. E. Hutchcroft,³⁶ D. J. Payne,³⁶ C. Touramanis,³⁶ A. J. Bevan,³⁷ F. Di Lodovico,³⁷ R. Sacco,³⁷ M. Sigamani,³⁷ G. Cowan,³⁸ S. Paramesvaran,³⁸ D. N. Brown,³⁹ C. L. Davis,³⁹ A. G. Denig,⁴⁰ M. Fritsch,⁴⁰ W. Gradl,⁴⁰ A. Hafner,⁴⁰ K. E. Alwyn,⁴¹ D. Bailey,⁴¹ R. J. Barlow,⁴¹ G. Jackson,⁴¹ G. D. Lafferty,⁴¹ R. Cenci,⁴² B. Hamilton,⁴² A. Jawahery,⁴² D. A. Roberts,⁴² G. Simi,⁴² C. Dallapiccola,⁴³ E. Salvati,⁴³ R. Cowan,⁴⁴ D. Dujmic,⁴⁴ G. Sciolla,⁴⁴ D. Lindemann,⁴⁵ P. M. Patel,⁴⁵ S. H. Robertson,⁴⁵ M. Schram,⁴⁵ P. Biassoni,^{46a,46b} A. Lazzaro,^{46a,46b} V. Lombardo,^{46a} F. Palombo,^{46a,46b} S. Stracka,^{46a,46b} L. Cremaldi,⁴⁷ R. Godang,^{47,‡} R. Kroeger,⁴⁷ P. Sonnek,⁴⁷ D. J. Summers,⁴⁷ X. Nguyen,⁴⁸ P. Taras,⁴⁸ G. De Nardo,^{49a,49b} D. Monorchio,^{49a,49b} G. Onorato,^{49a,49b} C. Sciacca,^{49a,49b} G. Raven,⁵⁰ H. L. Snoek,⁵⁰ C. P. Jessop,⁵¹ K. J. Knoepfel,⁵¹ J. M. LoSecco,⁵¹ W. F. Wang,⁵¹ K. Honscheid,⁵² R. Kass,⁵² J. P. Morris,⁵² J. Brau,⁵³ R. Frey,⁵³ N. B. Sinev,⁵³ D. Strom,⁵³ E. Torrence,⁵³ E. Feltresi,^{54a,54b} N. Gagliardi,^{54a,54b} M. Margoni,^{54a,54b} M. Morandin,^{54a} M. Posocco,^{54a} M. Rotondo,^{54a} F. Simonetto,^{54a,54b} R. Stroili,^{54a,54b} E. Ben-Haim,⁵⁵ M. Bomben,⁵⁵ G. R. Bonneaud,⁵⁵ H. Briand,⁵⁵ G. Calderini,⁵⁵ J. Chauveau,⁵⁵ O. Hamon,⁵⁵ Ph. Leruste,⁵⁵ G. Marchiori,⁵⁵ J. Ocariz,⁵⁵ S. Sitt,⁵⁵ M. Biasini,^{56a,56b} E. Manoni,^{56a,56b} A. Rossi,^{56a,56b} C. Angelini,^{57a,57b} G. Batignani,^{57a,57b} S. Bettarini,^{57a,57b} M. Carpinelli,^{57a,57b,§} G. Casarosa,^{57a,57b} A. Cervelli,^{57a,57b} F. Forti,^{57a,57b} M. A. Giorgi,^{57a,57b} A. Lusiani,^{57a,57c} N. Neri,^{57a,57b} B. Oberhof,^{57a,57b} E. Paoloni,^{57a,57b} A. Perez,^{57a} G. Rizzo,^{57a,57b} J. J. Walsh,^{57a} D. Lopes Pegna,⁵⁸ C. Lu,⁵⁸ J. Olsen,⁵⁸ A. J. S. Smith,⁵⁸ A. V. Telnov,⁵⁸ F. Anulli,^{59a} G. Cavoto,^{59a} R. Faccini,^{59a,59b} F. Ferrarotto,^{59a} F. Ferroni,^{59a,59b} M. Gaspero,^{59a,59b} L. Li Gioi,^{59a} M. A. Mazzoni,^{59a} G. Piredda,^{59a} C. Buenger,⁶⁰ T. Hartmann,⁶⁰ T. Leddig,⁶⁰ H. Schröder,⁶⁰ R. Waldi,⁶⁰ T. Adye,⁶¹ E. O. Olaiya,⁶¹ F. F. Wilson,⁶¹ S. Emery,⁶² G. Hamel de Monchenault,⁶² G. Vasseur,⁶² Ch. Yèche,⁶² D. Aston,⁶³ D. J. Bard,⁶³ R. Bartoldus,⁶³ J. F. Benitez,⁶³ C. Cartaro,⁶³ M. R. Convery,⁶³ J. Dorfan,⁶³ G. P. Dubois-Felsmann,⁶³ W. Dunwoodie,⁶³ R. C. Field,⁶³ M. Franco Sevilla,⁶³ B. G. Fulsom,⁶³ A. M. Gabareen,⁶³ M. T. Graham,⁶³ P. Grenier,⁶³ C. Hast,⁶³ W. R. Innes,⁶³ M. H. Kelsey,⁶³ H. Kim,⁶³ P. Kim,⁶³ M. L. Kocian,⁶³ D. W. G. S. Leith,⁶³ P. Lewis,⁶³ S. Li,⁶³ B. Lindquist,⁶³ S. Luitz,⁶³ V. Luth,⁶³ H. L. Lynch,⁶³ D. B. MacFarlane,⁶³ D. R. Muller,⁶³ H. Neal,⁶³ S. Nelson,⁶³ I. Ofte,⁶³ M. Perl,⁶³ T. Pulliam,⁶³ B. N. Ratcliff,⁶³ A. Roodman,⁶³ A. A. Salnikov,⁶³ V. Santoro,⁶³ R. H. Schindler,⁶³ A. Snyder,⁶³ D. Su,⁶³ M. K. Sullivan,⁶³ J. Va'vra,⁶³ A. P. Wagner,⁶³ M. Weaver,⁶³ W. J. Wisniewski,⁶³ M. Wittgen,⁶³ D. H. Wright,⁶³ H. W. Wulsin,⁶³ A. K. Yarritu,⁶³ C. C. Young,⁶³ V. Ziegler,⁶³ W. Park,⁶⁴ M. V. Purohit,⁶⁴ R. M. White,⁶⁴ J. R. Wilson,⁶⁴ A. Randle-Conde,⁶⁵ S. J. Sekula,⁶⁵ M. Bellis,⁶⁶ P. R. Burchat,⁶⁶ T. S. Miyashita,⁶⁶ M. S. Alam,⁶⁷ J. A. Ernst,⁶⁷ R. Gorodeisky,⁶⁸ N. Guttman,⁶⁸ D. R. Peimer,⁶⁸ A. Soffer,⁶⁸ P. Lund,⁶⁹ S. M. Spanier,⁶⁹ R. Eckmann,⁷⁰ J. L. Ritchie,⁷⁰ A. M. Ruland,⁷⁰ C. J. Schilling,⁷⁰ R. F. Schwitters,⁷⁰ B. C. Wray,⁷⁰ J. M. Izen,⁷¹ X. C. Lou,⁷¹ F. Bianchi,^{72a,72b} D. Gamba,^{72a,72b} L. Lanceri,^{73a,73b} L. Vitale,^{73a,73b}

N. Lopez-March,⁷⁴ F. Martinez-Vidal,⁷⁴ A. Oyanguren,⁷⁴ H. Ahmed,⁷⁵ J. Albert,⁷⁵ Sw. Banerjee,⁷⁵ H. H. F. Choi,⁷⁵ G. J. King,⁷⁵ R. Kowalewski,⁷⁵ M. J. Lewczuk,⁷⁵ C. Lindsay,⁷⁵ I. M. Nugent,⁷⁵ J. M. Roney,⁷⁵ R. J. Sobie,⁷⁵ T. J. Gershon,⁷⁶ P. F. Harrison,⁷⁶ T. E. Latham,⁷⁶ E. M. T. Puccio,⁷⁶ H. R. Band,⁷⁷ S. Dasu,⁷⁷ Y. Pan,⁷⁷ R. Prepost,⁷⁷ C. O. Vuosalo,⁷⁷ and S. L. Wu⁷⁷

(The BABAR Collaboration)

- ¹Laboratoire d'Annecy-le-Vieux de Physique des Particules (LAPP), Université de Savoie, CNRS/IN2P3, F-74941 Annecy-Le-Vieux, France
- ²Universitat de Barcelona, Facultat de Física, Departament ECM, E-08028 Barcelona, Spain
- ^{3a}INFN Sezione di Bari, I-70126 Bari, Italy
- ^{3b}Dipartimento di Fisica, Università di Bari, I-70126 Bari, Italy
- ⁴University of Bergen, Institute of Physics, N-5007 Bergen, Norway
- ⁵Lawrence Berkeley National Laboratory and University of California, Berkeley, California 94720, USA
- ⁶Ruhr Universität Bochum, Institut für Experimentalphysik 1, D-44780 Bochum, Germany
- ⁷University of British Columbia, Vancouver, British Columbia, Canada V6T 1Z1
- ⁸Brunel University, Uxbridge, Middlesex UB8 3PH, United Kingdom
- ⁹Budker Institute of Nuclear Physics, Novosibirsk 630090, Russia
- ¹⁰University of California at Irvine, Irvine, California 92697, USA
- ¹¹University of California at Riverside, Riverside, California 92521, USA
- ¹²University of California at Santa Barbara, Santa Barbara, California 93106, USA
- ¹³University of California at Santa Cruz, Institute for Particle Physics, Santa Cruz, California 95064, USA
- ¹⁴California Institute of Technology, Pasadena, California 91125, USA
- ¹⁵University of Cincinnati, Cincinnati, Ohio 45221, USA
- ¹⁶University of Colorado, Boulder, Colorado 80309, USA
- ¹⁷Colorado State University, Fort Collins, Colorado 80523, USA
- ¹⁸Technische Universität Dortmund, Fakultät Physik, D-44221 Dortmund, Germany
- ¹⁹Technische Universität Dresden, Institut für Kern- und Teilchenphysik, D-01062 Dresden, Germany
- ²⁰Laboratoire Leprince-Ringuet, CNRS/IN2P3, Ecole Polytechnique, F-91128 Palaiseau, France
- ²¹University of Edinburgh, Edinburgh EH9 3JZ, United Kingdom
- ^{22a}INFN Sezione di Ferrara, I-44100 Ferrara, Italy
- ^{22b}Dipartimento di Fisica, Università di Ferrara, I-44100 Ferrara, Italy
- ²³INFN Laboratori Nazionali di Frascati, I-00044 Frascati, Italy
- ^{24a}INFN Sezione di Genova, I-16146 Genova, Italy
- ^{24b}Dipartimento di Fisica, Università di Genova, I-16146 Genova, Italy
- ²⁵Indian Institute of Technology Guwahati, Guwahati, Assam, 781 039, India
- ²⁶Harvard University, Cambridge, Massachusetts 02138, USA
- ²⁷Harvey Mudd College, Claremont, California 91711
- ²⁸Universität Heidelberg, Physikalisches Institut, Philosophenweg 12, D-69120 Heidelberg, Germany
- ²⁹Humboldt-Universität zu Berlin, Institut für Physik, Newtonstr. 15, D-12489 Berlin, Germany
- ³⁰Imperial College London, London, SW7 2AZ, United Kingdom
- ³¹University of Iowa, Iowa City, Iowa 52242, USA
- ³²Iowa State University, Ames, Iowa 50011-3160, USA
- ³³Johns Hopkins University, Baltimore, Maryland 21218, USA
- ³⁴Laboratoire de l'Accélérateur Linéaire, IN2P3/CNRS et Université Paris-Sud 11, Centre Scientifique d'Orsay, B. P. 34, F-91898 Orsay Cedex, France
- ³⁵Lawrence Livermore National Laboratory, Livermore, California 94550, USA
- ³⁶University of Liverpool, Liverpool L69 7ZE, United Kingdom
- ³⁷Queen Mary, University of London, London, E1 4NS, United Kingdom
- ³⁸University of London, Royal Holloway and Bedford New College, Egham, Surrey TW20 0EX, United Kingdom
- ³⁹University of Louisville, Louisville, Kentucky 40292, USA
- ⁴⁰Johannes Gutenberg-Universität Mainz, Institut für Kernphysik, D-55099 Mainz, Germany
- ⁴¹University of Manchester, Manchester M13 9PL, United Kingdom
- ⁴²University of Maryland, College Park, Maryland 20742, USA
- ⁴³University of Massachusetts, Amherst, Massachusetts 01003, USA
- ⁴⁴Massachusetts Institute of Technology, Laboratory for Nuclear Science, Cambridge, Massachusetts 02139, USA
- ⁴⁵McGill University, Montréal, Québec, Canada H3A 2T8
- ^{46a}INFN Sezione di Milano, I-20133 Milano, Italy
- ^{46b}Dipartimento di Fisica, Università di Milano, I-20133 Milano, Italy

- ⁴⁷University of Mississippi, University, Mississippi 38677, USA
- ⁴⁸Université de Montréal, Physique des Particules, Montréal, Québec, Canada H3C 3J7
- ^{49a}INFN Sezione di Napoli, I-80126 Napoli, Italy
- ^{49b}Dipartimento di Scienze Fisiche, Università di Napoli Federico II, I-80126 Napoli, Italy
- ⁵⁰NIKHEF, National Institute for Nuclear Physics and High Energy Physics, NL-1009 DB Amsterdam, The Netherlands
- ⁵¹University of Notre Dame, Notre Dame, Indiana 46556, USA
- ⁵²Ohio State University, Columbus, Ohio 43210, USA
- ⁵³University of Oregon, Eugene, Oregon 97403, USA
- ^{54a}INFN Sezione di Padova, I-35131 Padova, Italy
- ^{54b}Dipartimento di Fisica, Università di Padova, I-35131 Padova, Italy
- ⁵⁵Laboratoire de Physique Nucléaire et de Hautes Energies, IN2P3/CNRS, Université Pierre et Marie Curie-Paris6, Université Denis Diderot-Paris7, F-75252 Paris, France
- ^{56a}INFN Sezione di Perugia, I-06100 Perugia, Italy
- ^{56b}Dipartimento di Fisica, Università di Perugia, I-06100 Perugia, Italy
- ^{57a}INFN Sezione di Pisa, I-56127 Pisa, Italy
- ^{57b}Dipartimento di Fisica, Università di Pisa, I-56127 Pisa, Italy
- ^{57c}Scuola Normale Superiore di Pisa, I-56127 Pisa, Italy
- ⁵⁸Princeton University, Princeton, New Jersey 08544, USA
- ^{59a}INFN Sezione di Roma, I-00185 Roma, Italy
- ^{59b}Dipartimento di Fisica, Università di Roma La Sapienza, I-00185 Roma, Italy
- ⁶⁰Universität Rostock, D-18051 Rostock, Germany
- ⁶¹Rutherford Appleton Laboratory, Chilton, Didcot, Oxon, OX11 0QX, United Kingdom
- ⁶²CEA, Irfu, SPP, Centre de Saclay, F-91191 Gif-sur-Yvette, France
- ⁶³SLAC National Accelerator Laboratory, Stanford, California 94309 USA
- ⁶⁴University of South Carolina, Columbia, South Carolina 29208, USA
- ⁶⁵Southern Methodist University, Dallas, Texas 75275, USA
- ⁶⁶Stanford University, Stanford, California 94305-4060, USA
- ⁶⁷State University of New York, Albany, New York 12222, USA
- ⁶⁸Tel Aviv University, School of Physics and Astronomy, Tel Aviv, 69978, Israel
- ⁶⁹University of Tennessee, Knoxville, Tennessee 37996, USA
- ⁷⁰University of Texas at Austin, Austin, Texas 78712, USA
- ⁷¹University of Texas at Dallas, Richardson, Texas 75083, USA
- ^{72a}INFN Sezione di Torino, I-10125 Torino, Italy
- ^{72b}Dipartimento di Fisica Sperimentale, Università di Torino, I-10125 Torino, Italy
- ^{73a}INFN Sezione di Trieste, I-34127 Trieste, Italy
- ^{73b}Dipartimento di Fisica, Università di Trieste, I-34127 Trieste, Italy
- ⁷⁴IFIC, Universitat de Valencia-CSIC, E-46071 Valencia, Spain
- ⁷⁵University of Victoria, Victoria, British Columbia, Canada V8W 3P6
- ⁷⁶Department of Physics, University of Warwick, Coventry CV4 7AL, United Kingdom
- ⁷⁷University of Wisconsin, Madison, Wisconsin 53706, USA

(Received 28 October 2011; published 18 May 2012)

We search for the rare decay of the D^0 meson to two photons, $D^0 \rightarrow \gamma\gamma$, and present a measurement of the branching fraction for a D^0 meson decaying to two neutral pions, $B(D^0 \rightarrow \pi^0\pi^0)$. The data sample analyzed corresponds to an integrated luminosity of 470.5 fb^{-1} collected by the *BABAR* detector at the PEP-II asymmetric-energy e^+e^- collider at SLAC. We place an upper limit on the branching fraction, $B(D^0 \rightarrow \gamma\gamma) < 2.2 \times 10^{-6}$, at 90% confidence level. This limit improves on the existing limit by an order of magnitude. We also find $B(D^0 \rightarrow \pi^0\pi^0) = (8.4 \pm 0.1 \pm 0.4 \pm 0.3) \times 10^{-4}$.

DOI: 10.1103/PhysRevD.85.091107

PACS numbers: 14.40.Lb, 12.15.Mm, 13.25.Ft

I. INTRODUCTION

In the standard model (SM) flavor-changing neutral currents (FCNC) are forbidden at tree level [1]. These decays are allowed at higher order and have been measured in the K and B meson systems [2]. In the charm sector, however, the small mass difference between down-type quarks of the first two families translates to a large suppression at the loop level from the GIM mechanism [1]. To

*Now at Temple University, Philadelphia, Pennsylvania 19122, USA

†Also with Università di Perugia, Dipartimento di Fisica, Perugia, Italy

‡Now at University of South Alabama, Mobile, Alabama 36688, USA

§Also with Università di Sassari, Sassari, Italy

date, measurements of radiative decays of charm mesons are consistent with results of theoretical calculations that include both short-distance and long-distance contributions and predict decay rates several orders of magnitude below the sensitivity of current experiments [3–8]. While these rates are small, it has been postulated that new physics (NP) processes can lead to significant enhancements [9].

In this paper, we report results of a search for the FCNC decay of the neutral D meson into two photons. The only previous study was conducted by the CLEO collaboration using 13.8 fb^{-1} [10]. Theoretical calculations predict that the decay $D^0 \rightarrow \gamma\gamma$ is dominated by long-distance effects. A calculation in the framework of Vector Meson Dominance (VMD) [11] yields

$$B(D^0 \rightarrow \gamma\gamma)^{(\text{VMD})} \simeq (3.5_{-2.6}^{+4.0}) \times 10^{-8}. \quad (1)$$

A separate calculation using heavy quark effective theory combined with chiral perturbation theory (HQ χ PT) [12] reveals a similar dominance of long-distance over short-distance (SD) effects, with the SD branching ratio estimated to be [11]

$$B(D^0 \rightarrow \gamma\gamma)^{(\text{SD})} \simeq 3 \times 10^{-11}. \quad (2)$$

In the context of the minimal supersymmetric standard model (MSSM), gluino exchange can enhance the SM rate by up to a factor of 200 [9]. The large number of charm decays in the *BABAR* dataset provide the opportunity to study this enhancement. A 200-fold increased rate would result in approximately 1370 events in the *BABAR* dataset (470.5 fb^{-1}) with only six events predicted from the theoretical SM branching fraction (3.5×10^{-8} , as determined in the VMD calculation.) A summary of the relevant branching fractions is shown in Table I.

In this paper we also report a new measurement of the branching fraction for the decay $D^0 \rightarrow \pi^0\pi^0$, which is the dominant background in the $D^0 \rightarrow \gamma\gamma$ analysis.

TABLE I. Summary of predictions and measured values or limits for branching fractions relevant to this analysis. The results presented in this paper are not included in this table.

Theoretical predictions		
Mode	Value	Reference
$D^0 \rightarrow \gamma\gamma$ (SM,VMD)	$\simeq (3.5_{-2.6}^{+4.0}) \times 10^{-8}$	Burdman [11]
$D^0 \rightarrow \gamma\gamma$ (SM, HQ χ PT)	$(1.0 \pm 0.5) \times 10^{-8}$	Fajfer [12]
$D^0 \rightarrow \gamma\gamma$ (MSSM)	6×10^{-6}	Prelovsek [9]
Experimental results		
Mode	Value	Reference
$D^0 \rightarrow \gamma\gamma$	$< 2.9 \times 10^{-5}$	Coan [10]
$D^0 \rightarrow \pi^0\pi^0$ (2006)	$(7.9 \pm 0.8) \times 10^{-4}$	Rubin [13]
$D^0 \rightarrow \pi^0\pi^0$ (2010)	$(8.1 \pm 0.5) \times 10^{-4}$	Mendez [14]
$D^0 \rightarrow K_S^0\pi^0$	$(1.22 \pm 0.05) \times 10^{-2}$	Nakamura [15]

II. THE *BABAR* DETECTOR AND DATASET

This analysis is based on a data sample corresponding to an integrated luminosity of 470.5 fb^{-1} collected by the *BABAR* detector at the SLAC PEP-II e^+e^- asymmetric-energy collider operating at e^+e^- center-of-mass (CM) energies of $\sqrt{s} = 10.58 \text{ GeV}$ and 10.54 GeV .

The *BABAR* detector is described in detail elsewhere [16]. Charged particle momenta and positions are measured with a five-layer double-sided silicon vertex tracker (SVT) and a 40-layer drift chamber (DCH). Charged hadron identification is provided by measurements of the ionization energy loss, dE/dx , in the tracking system and the Cherenkov angle obtained from a ring-imaging Cherenkov detector (DIRC). An electromagnetic calorimeter (EMC) consisting of 6580 CsI(Tl) crystals measures the energy deposited by electrons and photons. These detector elements are located inside the cryostat of a superconducting solenoidal magnet, which provides a 1.5 T magnetic field. The instrumented flux return (IFR) of the magnet allows discrimination of muons from pions.

A detailed Monte Carlo simulation (MC) of the *BABAR* detector based on GEANT 4 [17] is used to validate the analysis and determine the reconstruction efficiencies. We use simulated events to optimize the selection criteria by maximizing significance, defined as $N_S/\sqrt{N_S + N_B}$, where N_S and N_B denote the number of signal and background candidates in the MC simulation assuming a $D^0 \rightarrow \gamma\gamma$ branching fraction of 5.4×10^{-6} (5 times less than the CLEO collaboration upper limit). The background samples include $e^+e^- \rightarrow c\bar{c}$, $e^+e^- \rightarrow q\bar{q}$, $q = u, d$ or s , $e^+e^- \rightarrow B^0\bar{B}^0$, and $e^+e^- \rightarrow B^+B^-$ decay modes.

III. EVENT RECONSTRUCTION AND SELECTION

For the decay modes used in this study we require that the neutral D meson originates in the decay $D^{*+} \rightarrow D^0\pi^+$, which is referred to as a D^{*+} tag. (The inclusion of the charge conjugate modes is implied unless otherwise stated.) Without such a tag the signal is dominated by combinatoric background. To avoid uncertainties in the number of D^{*+} mesons in the *BABAR* dataset, we perform measurements of the $D^0 \rightarrow \gamma\gamma$ and $D^0 \rightarrow \pi^0\pi^0$ branching fractions relative to a well measured reference mode. The $D^0 \rightarrow K_S^0\pi^0$ decay is chosen for this purpose due to its large branching fraction of $(1.22 \pm 0.05)\%$ [15] and partial cancellation of systematic uncertainties in our measurements.

In the $D^0 \rightarrow \gamma\gamma$ analysis the D^0 candidate is formed by combining pairs of photon candidates. D^0 candidates are required to have an invariant mass between 1.7 and 2.1 GeV/c^2 for the $D^0 \rightarrow \gamma\gamma$ analysis and an invariant mass between 1.65 and 2.05 GeV/c^2 for the $D^0 \rightarrow \pi^0\pi^0$ analysis. A photon candidate is defined as energy deposited in the EMC, which is not associated with the trajectory of

any charged track and which exhibits the appropriate shower characteristics with a lateral moment [18] greater than 0.001. The photon candidates are selected to have CM energies between 0.74 and 4 GeV.

In the $D^0 \rightarrow \pi^0 \pi^0$ analysis two π^0 candidates each with CM momentum above 0.6 GeV/c are combined to form a D^0 candidate. The π^0 candidates are formed by combining two photon candidates with lateral moment less than 0.8. The list of π^0 candidates also includes single EMC clusters containing two adjacent photons (merged π^0).

The D^0 candidates for the $D^0 \rightarrow K_S^0 \pi^0$ reference mode are formed by combining a π^0 candidate as defined above with a K_S^0 candidate consistent with the decay $K_S^0 \rightarrow \pi^+ \pi^-$. The $\pi^+ \pi^-$ invariant mass is required to be between 0.491 and 0.505 GeV/c². To be selected as a K_S^0 candidate the decay length significance must be greater than 3, where the decay length significance is defined as the measured flight length divided by its estimated uncertainty.

In all modes, D^0 candidates are combined with π^+ candidates selected from tracks with CM momentum between 0.05 and 0.45 GeV/c. A kinematic fit is applied to the events, requiring the candidate D^0 invariant mass to be between 1.6 and 2.1 GeV/c². Both the D^0 and π^+ are constrained to originate from a common vertex within the beamspot to satisfy the D^{*+} tag requirement.

IV. BACKGROUND STUDIES

Backgrounds from B meson decays are removed by selecting D^{*+} candidates with CM momentum greater than 2.85 GeV/c in the case of $D^0 \rightarrow \gamma\gamma$ and greater than 2.4 GeV/c in the case of $D^0 \rightarrow \pi^0 \pi^0$. The difference reflects cuts optimized to separate MC samples.

In order to minimize systematic uncertainties the reference mode analysis was performed separately for each of the two signal modes, each time using identical criteria that were optimized for the respective signal mode. These selections result in 95% rejection of B meson decay modes. The $D^0 \rightarrow \gamma\gamma$ decay mode has significant backgrounds due to QED processes, which are largely removed by requiring that the total number of charged tracks in the event be greater than four and the number of neutral candidates in the event be greater than four.

The dominant background to $D^0 \rightarrow \gamma\gamma$ is due to $D^0 \rightarrow \pi^0 \pi^0$ decays. To remove this background, we implement a π^0 veto. From our sample of $D^0 \rightarrow \gamma\gamma$ candidates we reject all events in which one of the photons can be combined with any other photon candidate in the event to form a π^0 . This veto rejects 95% of the background and keeps 66% of the signal.

The $D^0 \rightarrow \gamma\gamma$ analysis signal efficiency is 6.1% with the corresponding reference mode ($D^0 \rightarrow K_S^0 \pi^0$, $K_S^0 \rightarrow \pi^+ \pi^-$) efficiency at 7.6%. The $D^0 \rightarrow \pi^0 \pi^0$ analysis signal and reference mode efficiencies are 15.2% and 12.0%, respectively.

V. FIT PROCEDURE AND RESULTS

For each of the three decay modes we determine the signal yield using unbinned maximum likelihood fits to the invariant mass distribution of D^0 candidates passing the above selection criteria. The overall probability distribution functions (PDFs) are sums of functions describing signal and background distributions obtained from the Monte Carlo simulation. The relative normalizations of these functions are free parameters while the individual shapes are fixed.

In the $D^0 \rightarrow \gamma\gamma$ analysis the signal PDF consists of a Crystal Ball [19] function and a bifurcated Gaussian distribution. The background PDF is a 2nd-order Chebychev polynomial and the $D^0 \rightarrow \pi^0 \pi^0$ background shape is described by a second Crystal Ball function. In the $D^0 \rightarrow \pi^0 \pi^0$ analysis the signal is described by a sum of a Gaussian, a bifurcated Gaussian, and a Crystal Ball function, and a background PDF described by a 3rd-order Chebychev polynomial.

The invariant $\gamma\gamma$ mass distribution obtained from the $D^0 \rightarrow \gamma\gamma$ analysis is shown in Fig. 1 together with projections of the likelihood fit and the individual signal and background combinations. The signal yield is -6 ± 15 ,

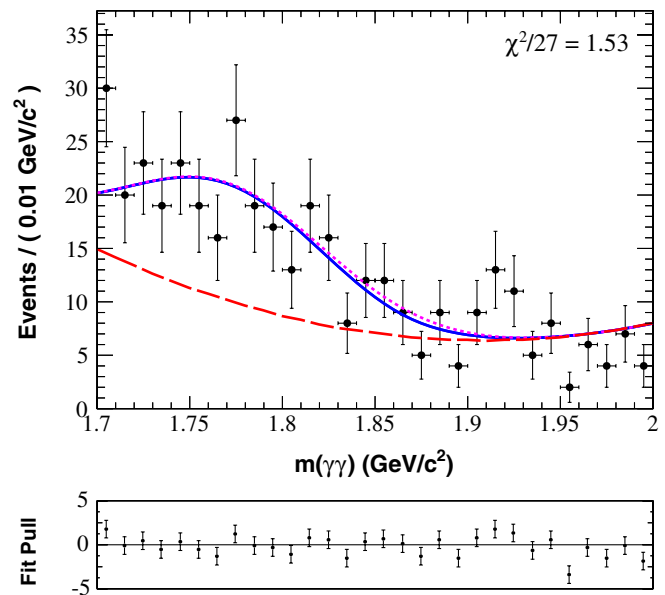


FIG. 1 (color online). The $\gamma\gamma$ mass distribution for $D^0 \rightarrow \gamma\gamma$ candidates in data (data points). The curves show the result of an unbinned maximum likelihood fit to the measured mass distribution. The solid blue curve corresponds to signal component resulting in a slight negative yield, the long-dash red curve corresponds to combinatoric background component, and the small-dash pink curve corresponds to the combinatoric background plus $D^0 \rightarrow \pi^0 \pi^0$ background shape. The χ^2 value is determined from binned data and is provided as a goodness-of-fit measure. The pull distribution shows differences between the data and the solid blue curve with values and errors normalized.

consistent with no $D^0 \rightarrow \gamma\gamma$ events. We convert this result to a branching fraction for $D^0 \rightarrow \gamma\gamma$ relative to the $D^0 \rightarrow K_S^0 \pi^0$ reference mode using

$$B(D^0 \rightarrow \gamma\gamma) = \frac{\frac{1}{\varepsilon_{\gamma\gamma}} N(D^0 \rightarrow \gamma\gamma)}{\frac{1}{\varepsilon_{K_S^0 \pi^0}} N(D^0 \rightarrow K_S^0 \pi^0)} \times B(D^0 \rightarrow K_S^0 \pi^0), \quad (3)$$

where N and ε are the yield and efficiency of the respective modes and $B(D^0 \rightarrow K_S^0 \pi^0)$ is the known $D^0 \rightarrow K_S^0 \pi^0; K_S^0 \rightarrow \pi^+ \pi^-$ branching fraction [15]. In this analysis the $D^0 \rightarrow K_S^0 \pi^0$ signal yield is 126599 ± 568 events. We find $B(D^0 \rightarrow \gamma\gamma) = (-0.49 \pm 1.23 \pm 0.02) \times 10^{-6}$ where the errors are the statistical uncertainty and the uncertainty in the reference mode branching fraction, respectively.

The invariant mass distribution for events in the $D^0 \rightarrow \pi^0 \pi^0$ analysis is shown in Fig. 2. The signal yield for $D^0 \rightarrow \pi^0 \pi^0$ is 26010 ± 304 events. For $D^0 \rightarrow K_S^0 \pi^0$ (mass distribution not shown) the signal yield is 207538 ± 1143 events. Adjusting Eq. (3) for the $D^0 \rightarrow \pi^0 \pi^0$ case we convert this yield to a branching fraction and find $B(D^0 \rightarrow \pi^0 \pi^0) = (8.4 \pm 0.1 \pm 0.3) \times 10^{-4}$. The first error denotes the statistical uncertainty and the second error reflects the uncertainties in the reference mode branching fraction.

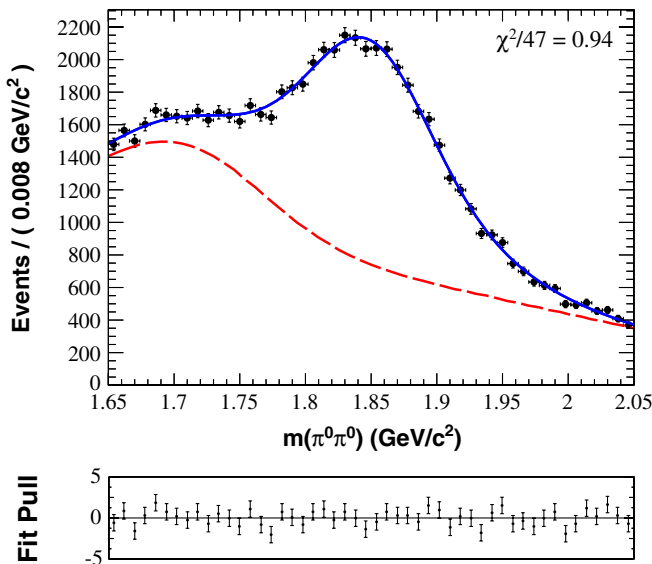


FIG. 2 (color online). The $\pi^0 \pi^0$ mass distribution for $D^0 \rightarrow \pi^0 \pi^0$ candidates in data (data points). The curves show the result of the unbinned maximum likelihood fit to the measured mass distribution. The solid blue curve corresponds to the full PDF including the signal and the dashed red curve corresponds to the combinatoric background. The χ^2 value is determined from binned data and is provided as a goodness-of-fit measure. The pull distribution shows differences between the data and the solid blue curve with values and errors normalized.

VI. SYSTEMATIC UNCERTAINTIES

Several systematic uncertainties cancel partially or completely when the branching fraction is measured with respect to the $D^0 \rightarrow K_S^0 \pi^0$ reference mode. The uncertainty in tracking efficiency and vertexing 1.39%. The uncertainty due to photon reconstruction efficiency in the ratio of the signal mode branching fraction to the reference mode branching fraction is 3.0% and 0.6% for the $D^0 \rightarrow \pi^0 \pi^0$ and $D^0 \rightarrow \gamma\gamma$ analyses, respectively.

In order to account for the uncertainty arising from fixed PDF shapes, the parameters determined from the Monte Carlo simulation, are varied by random amounts sampled from the covariance matrix retaining correlations among parameters. The values of these parameters are fixed and the resulting PDF is fit to data allowing the yield to float, the 1σ width of the obtained signal yield distribution is taken as the systematic uncertainty. In the $D^0 \rightarrow \pi^0 \pi^0$ analysis, fixing the signal and combinatoric background shapes results in 0.20% and 0.80% systematic uncertainties, respectively. Fixing the $D^0 \rightarrow K_S^0 \pi^0$ signal and background shapes for the reference mode results in 0.17% and 0.63% systematic uncertainties, respectively.

Potential differences in π^0 veto efficiencies between data and the Monte Carlo simulation are estimated using a sample of candidates for the physically forbidden decay $D^0 \rightarrow K_S^0 \gamma$. The difference in the ratios of numbers of candidates before and after the veto between data and the Monte Carlo simulation is taken as the systematic uncertainty. We measure the difference as a function of the number of photons in the event and as a function of the photon energy. In all cases, the variations are found to be less than or equal to 1.8%.

In order to account for imperfect modeling of D^{*+} hadronization, a 4% correction is applied to the MC for normalized momenta, $x = p(D^{*+})/p_{\max}(D^{*+})$, within the region $x = 0.575$ to $x = 0.7$ to match cross section measurements made by the CLEO collaboration [20]. We calculate the ratios of signal efficiencies ($\varepsilon_{D^0 \rightarrow \gamma\gamma} / \varepsilon_{D^0 \rightarrow K_S^0 \pi^0}$, $\varepsilon_{D^0 \rightarrow \pi^0 \pi^0} / \varepsilon_{D^0 \rightarrow K_S^0 \pi^0}$) with and without this correction applied to the MC and determine systematic uncertainties of 0.02% and 0.03% for the $D^0 \rightarrow \gamma\gamma$ and $D^0 \rightarrow \pi^0 \pi^0$ modes, respectively, due to this correction.

To account for systematic uncertainties due to applying a particular set of selection criteria, we vary the selection criteria and recalculate the results. The reconstruction efficiency is determined from MC and the efficiency-corrected yield is measured from data when each set of selection criteria is applied. These yields are found to be distributed normally and the standard deviation is taken to be the systematic uncertainty. Choosing particular event selections for the $D^0 \rightarrow \pi^0 \pi^0$ and $D^0 \rightarrow K_S^0 \pi^0$ studies results in systematic uncertainties of 2.50% and 0.76%, respectively.

TABLE II. Summary of systematic uncertainties, σ , for each mode.

Source of Systematic Uncertainty	$\sigma(D^0 \rightarrow \gamma\gamma)$ (%)	$\sigma(D^0 \rightarrow \pi^0\pi^0)$ (%)
Tracking (K_S^0) and Vertexing	1.39	1.39
Photon Reconstruction	0.60	3.0
π^0 Veto	1.8	-
D^{*+} Hadronization	0.02	0.03
Signal Shape	^a	0.20
Background Shape	^a	0.80
Selection Criteria	^a	2.5
$D^0 \rightarrow K_S^0\pi^0$ Signal Shape	0.10	0.17
$D^0 \rightarrow K_S^0\pi^0$ Background Shape	0.53	0.63
$D^0 \rightarrow K_S^0\pi^0$ Selection Criteria	0.76	0.76
Total Systematic Uncertainty	^a	4.3

^aThese sources of systematic uncertainty are assessed in a combined Monte Carlo simulation study. See text for details.

The systematic uncertainties are summarized in Table II. For the $D^0 \rightarrow \pi^0\pi^0$ mode a total systematic uncertainty of 4.2% is obtained by adding all contributions in quadrature.

For the $D^0 \rightarrow \gamma\gamma$ analysis we combine all systematic uncertainties with the statistical uncertainties in the upper-limit calculation. In a Monte Carlo simulation study we generate event samples using the complete background PDF from the data fit and repeat the branching fraction calculation 14000 times varying all sources of systematic uncertainties in the process. For each branching fraction calculation the selection values on the continuous variables are varied within ranges established from the $D^0 \rightarrow \pi^0\pi^0$ analysis. In each calculation the parameters of the signal and background PDFs are varied within their uncertainties while fully accounting for the correlations among them. Systematic uncertainties such as tracking, photon reconstruction, π^0 veto, and D^{*+} hadronization are added in quadrature and the $D^0 \rightarrow \gamma\gamma$ signal efficiency is varied randomly according to a normal distribution with a width equal to this total uncertainty. To account for the uncertainty in the branching fraction of the $D^0 \rightarrow K_S^0\pi^0$ refer-

ence mode, the nominal value is varied randomly according to a normal distribution with a width equal to the established $D^0 \rightarrow K_S^0\pi^0$ branching fraction uncertainty [15]. The resulting distribution of $B(D^0 \rightarrow \gamma\gamma)$ branching fractions is shown in Fig. 3.

Integrating this distribution to 90% of the area with $B(D^0 \rightarrow \gamma\gamma) > 0$ gives us the expected sensitivity of our analysis. We find

$$B(D^0 \rightarrow \gamma\gamma) < 2.4 \times 10^{-6} \quad (4)$$

at 90% confidence level.

VII. RESULTS

In this paper, we present a new measurement for the branching fraction for a D^0 meson decaying to two neutral pions:

$$B(D^0 \rightarrow \pi^0\pi^0) = (8.4 \pm 0.1 \pm 0.4 \pm 0.3) \times 10^{-4}, \quad (5)$$

where the errors denote the statistical, systematic, and reference mode branching fraction uncertainties, respectively.

We also report the result of a search for the decay of a neutral D meson to two photons. The observed yield is -6 ± 15 consistent with no $D^0 \rightarrow \gamma\gamma$ events. Our analysis has an expected sensitivity of $B(D^0 \rightarrow \gamma\gamma) < 2.4 \times 10^{-6}$ at 90% confidence level. In order to obtain an upper limit for $B(D^0 \rightarrow \gamma\gamma)$ we repeat the sensitivity study described in Sec. VI with the signal yield set to the measured value of -6 instead of 0 and find

$$B(D^0 \rightarrow \gamma\gamma) < 2.2 \times 10^{-6} \quad (6)$$

at 90% confidence level.

This result is consistent with our expected sensitivity and with SM expectations. As stated earlier, gluino exchange has been postulated to possibly enhance the SM rate by up to a factor of 200 [9]. Based on the upper limit of

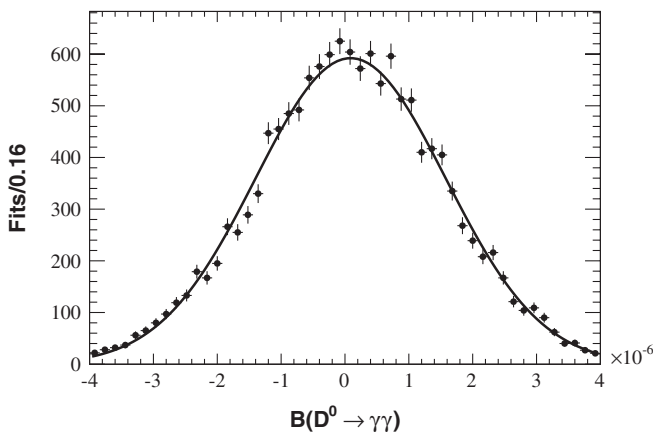


FIG. 3. Distribution of branching fraction calculations when varying all sources of uncertainty.

the branching fraction for $D^0 \rightarrow \gamma\gamma$ presented in this paper, the enhancement of the rate over the expected SM rate cannot exceed a factor of 70.

ACKNOWLEDGMENTS

We are grateful for the extraordinary contributions of our PEP-II colleagues in achieving the excellent luminosity and machine conditions that have made this work possible. The success of this project also relies critically on the expertise and dedication of the computing organizations that support *BABAR*. The collaborating institutions wish to thank S.L.A.C. for its support and the kind hospitality extended to them. This work is supported by the U.S. Department of Energy and National Science Foundation, the Natural Sciences and Engineering

Research Council (Canada), the Commissariat à l’Energie Atomique and Institut National de Physique Nucléaire et de Physique des Particules (France), the Bundesministerium für Bildung und Forschung and Deutsche Forschungsgemeinschaft (Germany), the Istituto Nazionale di Fisica Nucleare (Italy), the Foundation for Fundamental Research on Matter (The Netherlands), the Research Council of Norway, the Ministry of Education and Science of the Russian Federation, Ministerio de Ciencia e Innovación (Spain), and the Science and Technology Facilities Council (United Kingdom). Individuals have received support from the Marie-Curie IEF program (European Union), the A.P. Sloan Foundation (USA) and the Binational Science Foundation (USA-Israel).

-
- [1] S.L. Glashow, J. Iliopoulos, and L. Maiani, *Phys. Rev. D* **2**, 1285 (1970).
 - [2] T. Hurth, *Rev. Mod. Phys.* **75**, 1159 (2003).
 - [3] M. K. Gaillard and B. W. Lee, *Phys. Rev. D* **10**, 897 (1974).
 - [4] E. Ma and A. Pramudita, *Phys. Rev. D* **24**, 2476 (1981).
 - [5] J. O. Eeg, B. Nizic, and I. Picek, *Phys. Lett. B* **244**, 513 (1990).
 - [6] J. L. Goity, *Z. Phys. C* **34**, 341 (1987).
 - [7] G. D’Ambrosio and D. Espriu, *Phys. Lett. B* **175**, 237 (1986).
 - [8] J. Kambor and B.R. Holstein, *Phys. Rev. D* **49**, 2346 (1994).
 - [9] S. Prelovsek and D. Wyler, *Phys. Lett. B* **500**, 304 (2001).
 - [10] T.E. Coan *et al.* (CLEO Collaboration), *Phys. Rev. Lett.* **90**, 101801 (2003).
 - [11] G. Burdman, E. Golowich, J. A. Hewett, and S. Pakvasa, *Phys. Rev. D* **66**, 014009 (2002).
 - [12] S. Fajfer, P. Singer, and J. Zupan, *Phys. Rev. D* **64**, 074008 (2001).
 - [13] P. Rubin *et al.* (CLEO Collaboration), *Phys. Rev. Lett.* **96**, 081802 (2006).
 - [14] H. Mendez, *Phys. Rev. D* **81** (2010), ISSN, <http://prd.aps.org/abstract/PRD/v81/i5/e052013>.
 - [15] K. Nakamura *et al.* (Particle Data Group), *J. Phys. G* **37**, 075021 (2010).
 - [16] B. Aubert *et al.* (*BABAR* Collaboration), *Nucl. Instrum. Methods Phys. Res., Sect. A* **479**, 1 (2002).
 - [17] S. Agostinelli *et al.*, *Nucl. Instrum. Methods Phys. Res., Sect. A* **506**, 250 (2003).
 - [18] A. Drescher *et al.*, *Nucl. Instrum. Methods Phys. Res., Sect. A* **237**, 464 (1985), ISSN, <http://www.sciencedirect.com/science/article/B6TJM-473M9SS-FC/2/27e88b2ceddd74f2e71151ce5c9613c2>.
 - [19] J.E. Gaiser *et al.*, *Phys. Rev. D* **34**, 711 (1986).
 - [20] G. Colangelo and P. Nason, *Phys. Lett. B* **285**, 167 (1992), ISSN, <http://www.sciencedirect.com/science/article/pii/0370269392913173>.